A Summary of the GBT Optics Design

R. Norrod and S. Srikanth

March 1996

A Summary of the GBT Optics Design

R. Norrod and S. Srikanth

March 1996

1.0 Primary Reflector

The primary reflector of the GBT will be an offset paraboloid of 100-meter projected aperture. The offset design provides an aperture that is completely free of blockage. The following paragraphs define the coordinate systems and nomenclature used throughout this document.

A cartesian coordinate system is defined with origin at the focus of the parabolid (F_o). As illustrated in Figure 1-1, y is positive upwards, z to the right, and the x-axis, as determined by the right-hand rule, is positive into the paper. A point P can be described with (x, y, z) coordinates or with spherical coordinates (r, ϕ, Θ) defined relative to (x, y, z) in the usual way. In the following, all dimensions are in meters and angles in degrees, unless otherwise noted.

The surface of the primary reflector is defined by the equation of the parent paraboloid:

$$x^2 + y^2 = 4f(f - z)$$

where

$$f = F_o V_o .$$

V_o is the vertex of the paraboloid. The edge of the primary reflector is defined by the intersection of the parent paraboloid with a cone defined by the angles Θ_o and Θ^*, indicated in Figure 1-1.

The following parameter values have been chosen for the primary reflector surface:

$$R = 50$$

$$Y_c = 54$$

$$f = 60$$

Given these values, then:

$$\Theta_o = 42.825°$$

$$\Theta^* = 39.005°$$

The point I_C, the center of the projected aperture on the reflector surface, is located at:

I_C: $r = 72.150$, $\phi = 90$, $\Theta = 48.455$

$x = 0$, $y = Y_C = 54$, $z = 47.850$

2.0 Prime Focus Operation

A prime focus receiver mount will be provided for receiver and feed combinations weighing up to 1500 pounds. The mount will be capable of rotating

the receiver through 410 degrees at rates up to 1 RPM. Feed translation along its boresight axis of 50 inches will be provided. The feed boresight will be along a line tilted 45.5 degrees with respect to the paraboloid axis. Receiver motion orthogonal to this line and in the Y-Z plane will be provided to track the focal point motion due to gravitional deformations. These motions, together with specifications on speeds and repeatability, are further described in Figure 2-1.

The prime focus receiver mount is located on a boom that swings into position in front of the subreflector for prime focus operation. Deployment or retraction of the prime focus boom will take approximately five minutes, and may be done remotely.

3.0 Secondary Focus Operation

Secondary focus receivers will be supported for operation above approximately 1 GHz. The secondary focus feeds will be mounted along a circle on a rotating turret and any one of the feeds can be selected to be at the focus. It will be possible to switch between prime and secondary focus operations without manual intervention and within a few minutes.

3.1 Subreflector Mount

It is known that the primary reflector focal point will wander relative to the subreflector mounting points due to gravitational and thermal deformations of the primary reflector and the feed support arm. The subreflector mount will be capable of tracking the focal point motion. Five degrees of motion will be provided in the subreflector mount; three translations and two tilts. These motions, together with specifications on speeds and repeatability, are further described in Figure 3-1.

3.2 Subreflector

A gregorian subreflector design has been selected. The subreflector is an offset portion of an ellipsoid of revolution. The ellipsoid axis is tilted as described by Dragone (BSTJ, Sept. 1978), Mizugutch, et al. (AP Symposium, 1976), and Sletten (Reflector and Lens Antennas, Aertech House) in order to minimize cross-polarization due to asymmety of the primary reflector. In order for this technique to achieve -40 dB cross-pol, the subreflector should be approximately 25 wavelengths across [Adatia, IEEE Ant. & Prop. Symp. Digest, May 1978, p235]. For the GBT design this limit is satisfied at frequencies above 1 GHz.

The following parameters have been selected for the subreflector:

$$e = 0.528$$

$$C = 11$$

$$\alpha = 17.899$$

$$ß = 5.570$$

$$\Theta_H = 14.99$$

where e is the eccentricity of the parent ellipsoid, and the other parameters are identified in Figure 3-2. The subreflector surface is defined by the parent ellipsoid, and the edge by the intersection of the ellipsoid and a cone with vertex at F_1, axis on the line F_1I_1, and half-angle Θ_H.

The coordinates of the secondary focus (F_1) are:

F_1: $r = 11$, $\phi = -90°$, $\Theta = ß = 5.570$

$x = 0$, $y = -1.068$, $z = 10.948$

The subreflector size is 7.55 x 7.95 meters. The distance $F_1 I_1$ is 15.10 meters. The distance F_oI_1 is 5.73 meters. The effective focal length from the secondary focus is 190 meters.

The subreflector surface accuracy is specified to be 100 micrometers RMS. The antenna contractor is constructing the subreflector using a panel and backup structure approach. The subreflector panels will be constructed of aluminum, with a skin and frame technique similar to the primary reflector panels. The subreflector backup structure will be also be constructed of aluminum. Forty panels are used to form the subreflector surface.

4.0 POINTING COEFFICIENTS

At the secondary focus, the pointing change for lateral feed offsets is approximately 0.45 HPBW per wavelength of offset. Table 4-1 shows the calculated coefficients for the GBT. Figure 4-1 describes the coordinate system used in determining these coefficients. The coefficients were calculated using a geometrical theory of diffraction analysis of the dual reflector geometry.

5.0 PERFORMANCE ESTIMATES

Estimates of the prime focus efficiency were done using software based on aperture integration and geometric theory of diffraction. At a frequency of 800 MHz, the aperture efficiency and spillover were calculated for various feed horn flare angles. In Figure 5-1, this data is plotted, giving the prime focus aperture efficiency divided by system noise versus horn flare angle, for various values of receiver noise. Based on these results, a horn semi-flare angle of 30° was selected, giving a reflector edge taper of -22dB. The resulting aperture efficiency is 60% and the spillover temperature is approximately 5K.

Dual reflector analysis was carried out using Jacobi Bessel - Geometric Theory of Diffraction software provided by the Jet Propulsion Laboratory. Both of

the above account for the edge diffraction effects of the reflectors. The ratio of gain/system temperature (G/T) was calculated for different feed tapers at the edge of the subreflector. The results at 1.42 GHz and 5.00 GHz are shown in Figures 5-2 and 5-3. At 1.42 GHz, G/T peaks at -18dB feed taper while at 5.00 GHz, G/T peaks at -15dB. An L-band feed with -18dB taper would be too large and heavy for the feed turret and hence -15dB taper feeds will be used for all frequencies.

Table 5-1 gives the efficiency estimates at 1.42, 5.00 and 20.00 GHz. E_{main} and E_{sub} are spillover efficiencies at the primary reflector and subreflector, respectively. E_{ill} is the illumination efficiency. No estimate of the miscellaneous losses such as VSWR is available. E_{tot} is the peak total aperture efficiency exclusive of a surface efficiency term.

The prime focus beam pattern at 800 MHz is shown in Figure 5-4. The first sidelobe is about -28dB below the beam peak. Figure 5-5 shows the beam patterns of the gregorian geometry at 5 GHz. The first sidelobe is about -27dB down from the main beam peak.

The beam scanning performance of the dual reflector geometry was studied at 1.42 GHz and 5.00 GHz. The optimum feed location for a given scan of the telescope beam was determined by tracing the caustics as described by Sletten (Reflector And Lens Antennas). Table 5-2 lists loss in gain, ratio of beamwidths

of scanned to unscanned beams and first sidelobe level for 2.8 and 6 beamwidth scans at 1.42 GHz and for 2.8, 6 and 10 beamwidth scans at 5.00 GHz. These are given for both symmetric and asymmetric planes of the offset telescope. Scanned far-field patterns in the symmetric plane are shown in Figures 5-6 and 5-7.

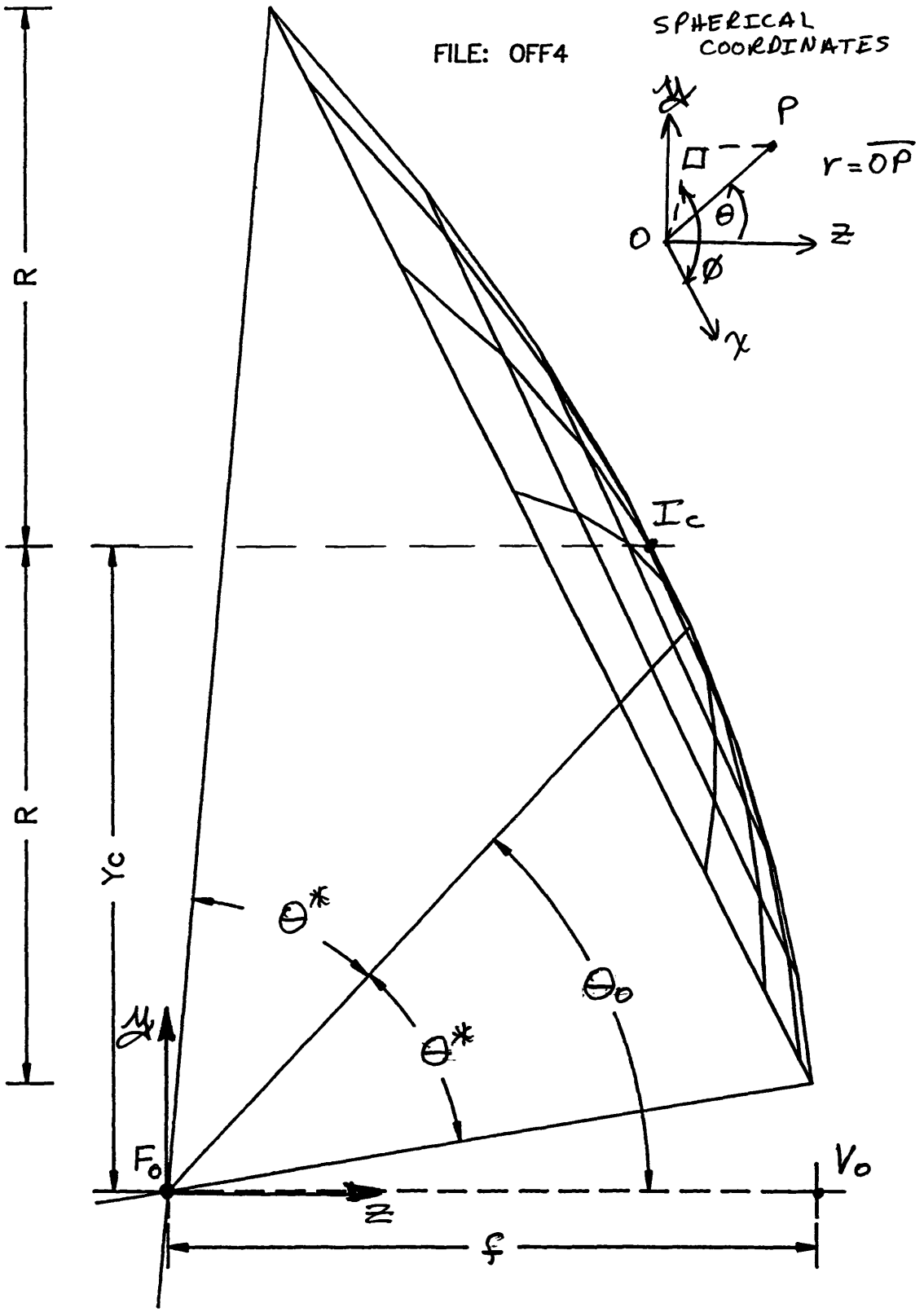

Figure 1-1
GBT Primary Reflector Geometry

PRIME FOCUS RECEIVER MOUNT
ADJUSTMENTS:

TRANSLATION ON Yp
RANGE: 50 in
SPEED: 6 in/min
REPEATABILITY: ± 0.03 in

TRANSLATION ON Xp
RANGE: 37 in
SPEED: 12 in/min
REPEATABILITY: 0.1 in

ROTATION ABOUT Yp (POLARIZATION)
RANGE: ± 205°
SPEED: 1 rpm
REPEATABILITY: ± 6 arcmin

FIGURE 2–1
GBT Prime Focus Receiver Mount
Adjustment Specifications

NOTES:
1. Xp AND Yp LIE IN ANTENNA PLANE OF SYMMETRY.
2. REF: RSI DWG 121039

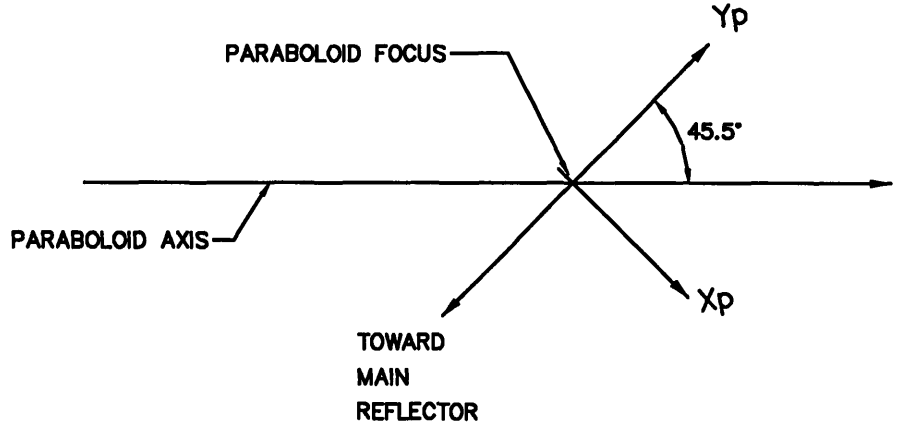

SUBREFLECTOR
ADJUSTMENTS:

TRANSLATION ON Ys
  RANGE:
    +12 in
    −24 in
SPEED: 24 in/min
REPEATABILITY: ± 0.002 in

TRANSLATION ON Xs
  RANGE: ±10 in
  SPEED: 24 in/min
  REPEATABILITY: ± 0.002 in

TRANSLATION ON Zs
  RANGE: ± 1 IN
  SPEED: 24 in/min
  REPEATABILITY: ± 0.002 IN

TILT ABOUT Xn
  RANGE: ± 1.5°
  SPEED: 1 °/sec
  REPEATABILITY: ± 3 arcsec

TILT ABOUT Zs
  RANGE: ± 0.5°
  SPEED: 0.25 °/sec
  REPEATABILITY: ± 3 ARCSEC

FIGURE 3–1
GBT Subreflector Mount
Adjustment Specifications

NOTES:
1. Xs AND Ys LIE IN ANTENNA PLANE OF SYMMETRY.
2. Zs IS PERPENDICULAR TO Xs AND Ys.
3. REF: RSI DWG 121038

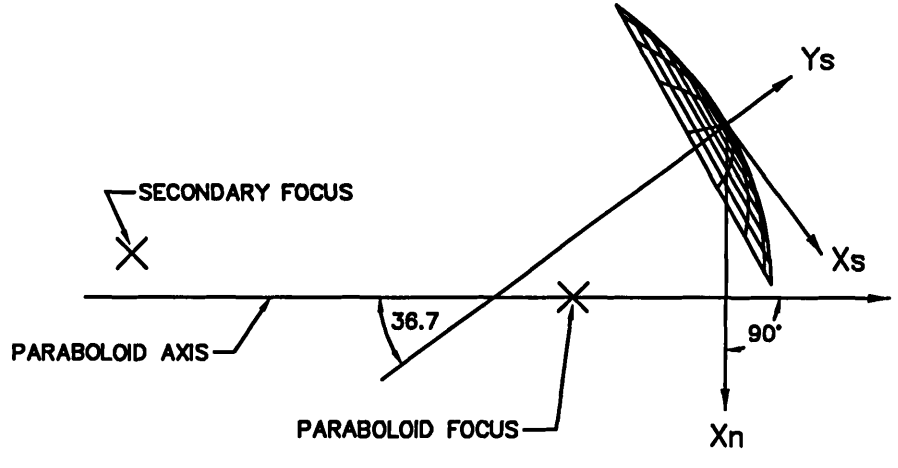

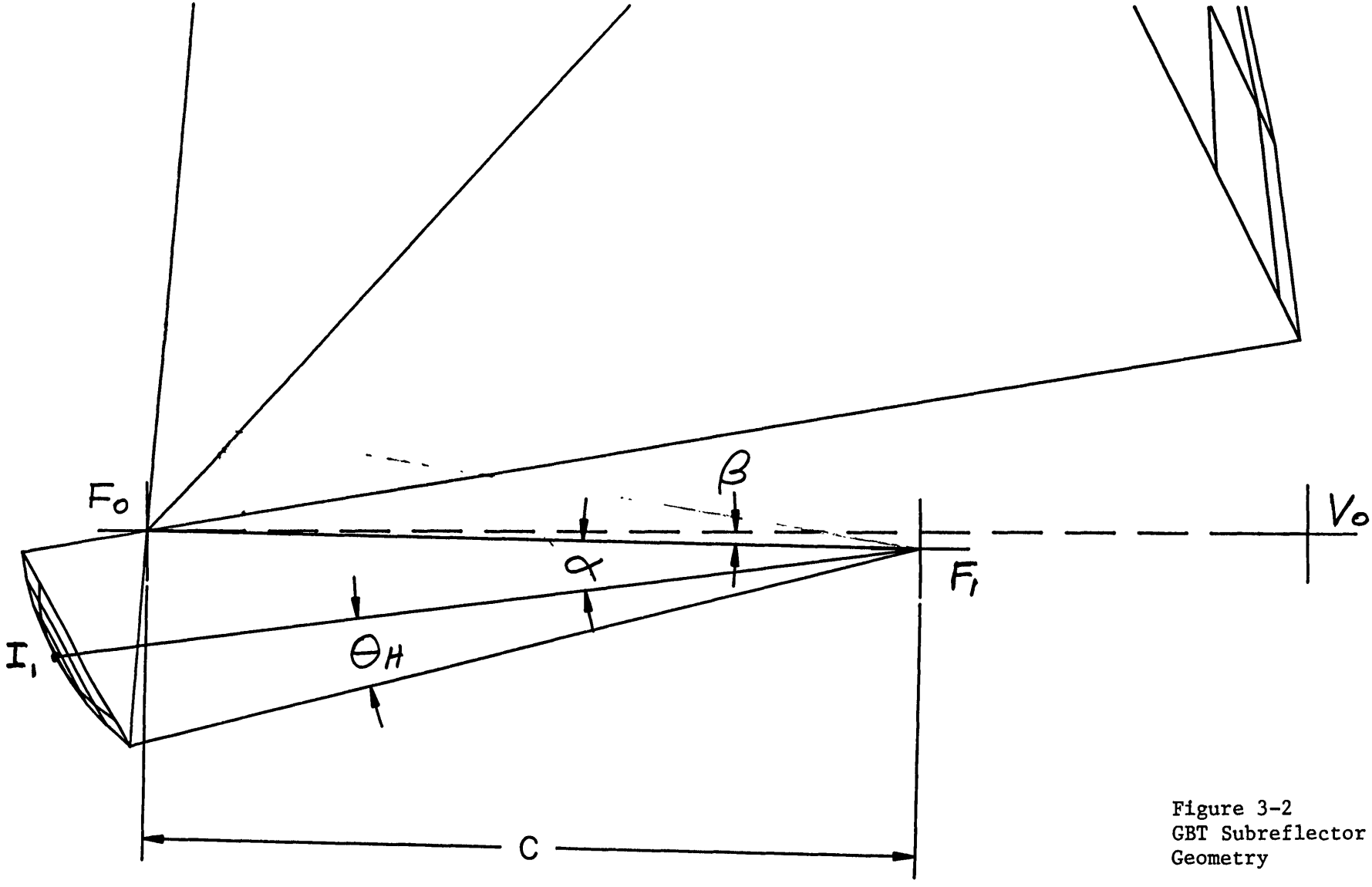

Figure 3-2
GBT Subreflector
Geometry

Table 4-1

GBT Pointing Coefficients

Translation/Rotation	arcsec arcsec	arcsec mm	arcsec inch
Subreflector Rotation about X axis	0.1504		
Subreflector +Y shift		2.908	73.87
Subreflector +Z shift		2.125	53.96
Feed +Y shift		-1.052	-26.72
Feed +Z shift		-0.248	- 6.28
Parabola Rotation about X axis	1.5490		
Parabola +Y shift		-1.877	-47.68
Parabola +Z shift		-1.898	-48.20
Beam Deviation Factor in YZ plane - Prime Focus	0.9280		
Subreflector Rotation about Y axis	0.1336		
Subreflector +X shift		-3.775	-95.88
Feed +X shift		1.052	26.72
Parabola Rotation about Y axis	1.7710		
Parabola +X shift		2.681	68.11
Beam Deviation Factor in XZ plane - Prime Focus	0.9400		
Change in Focal Length		-1.898	-48.20

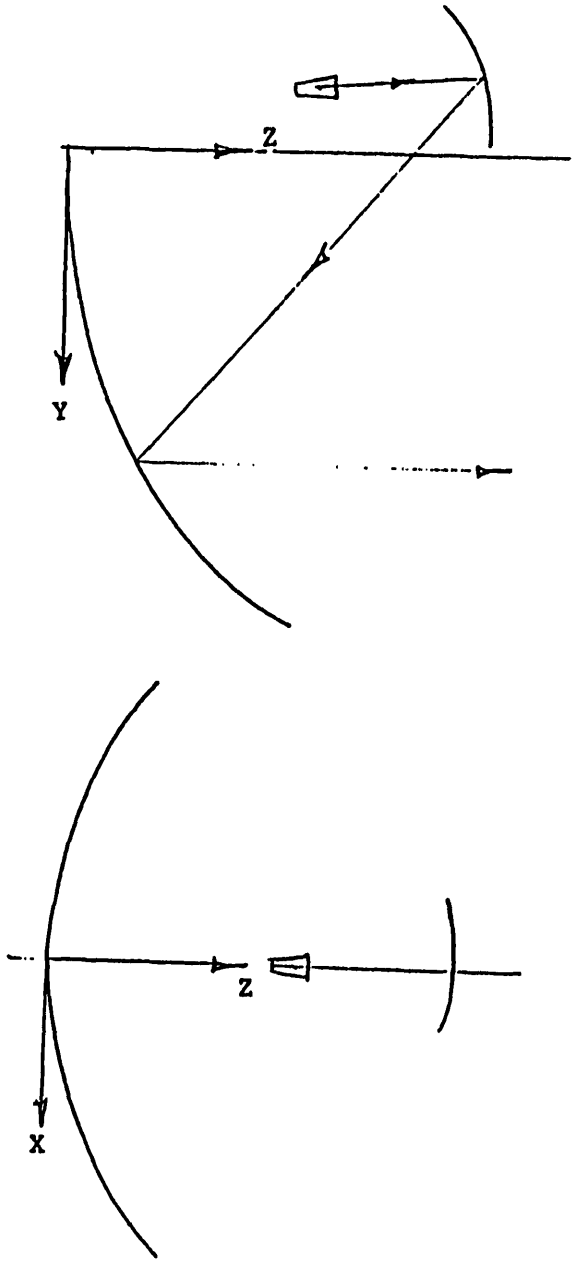

a) Translations

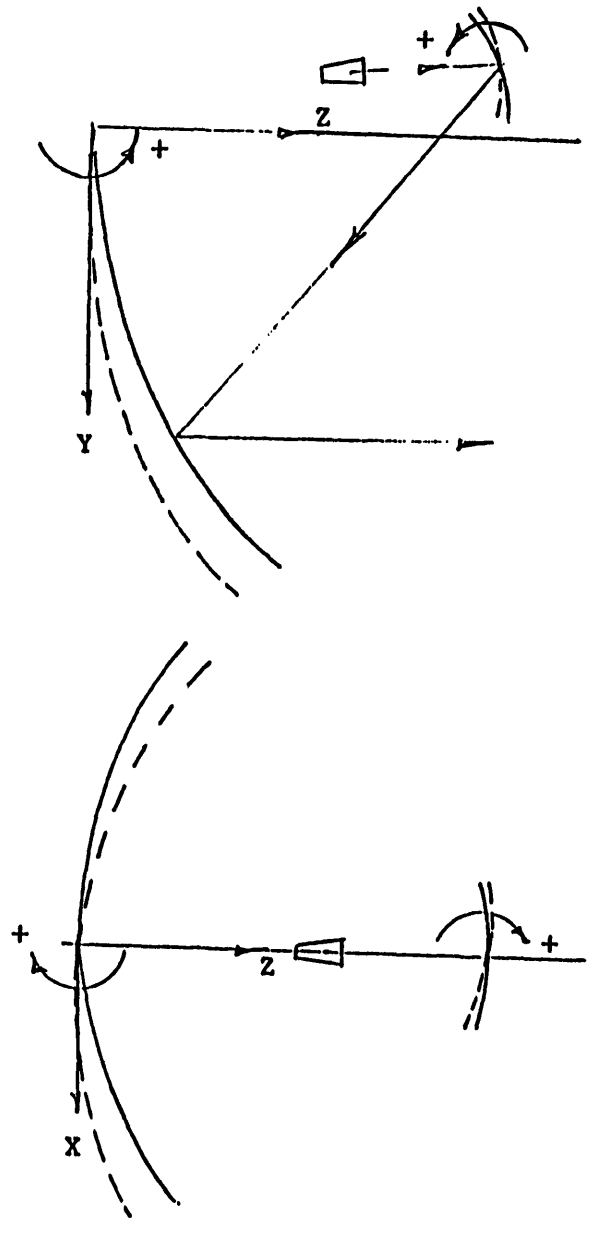

b) Rotations

Figure 4-1
Coordinate Systems
used in Calculation
of Pointing
Coefficients

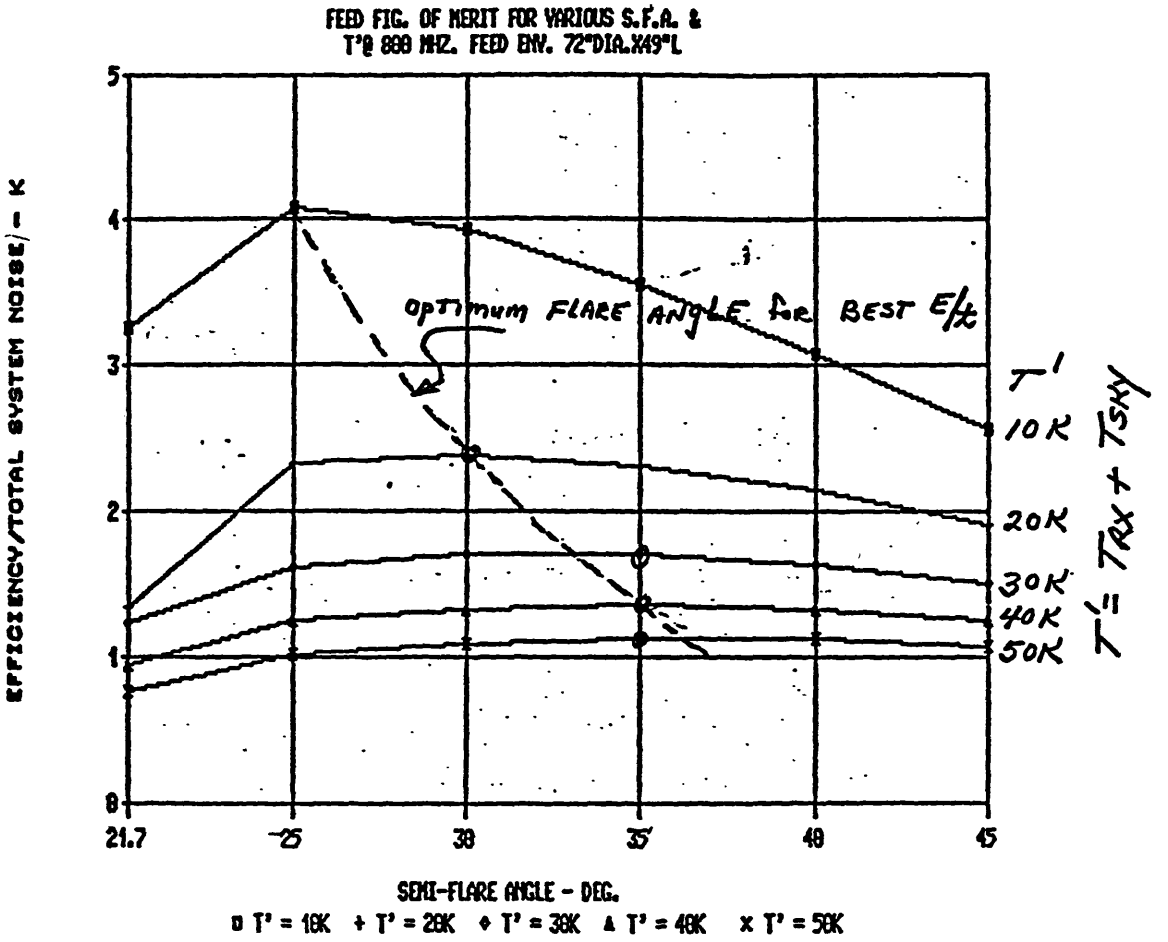

Figure 5-1
Prime Focus Feed
Figure of Merit

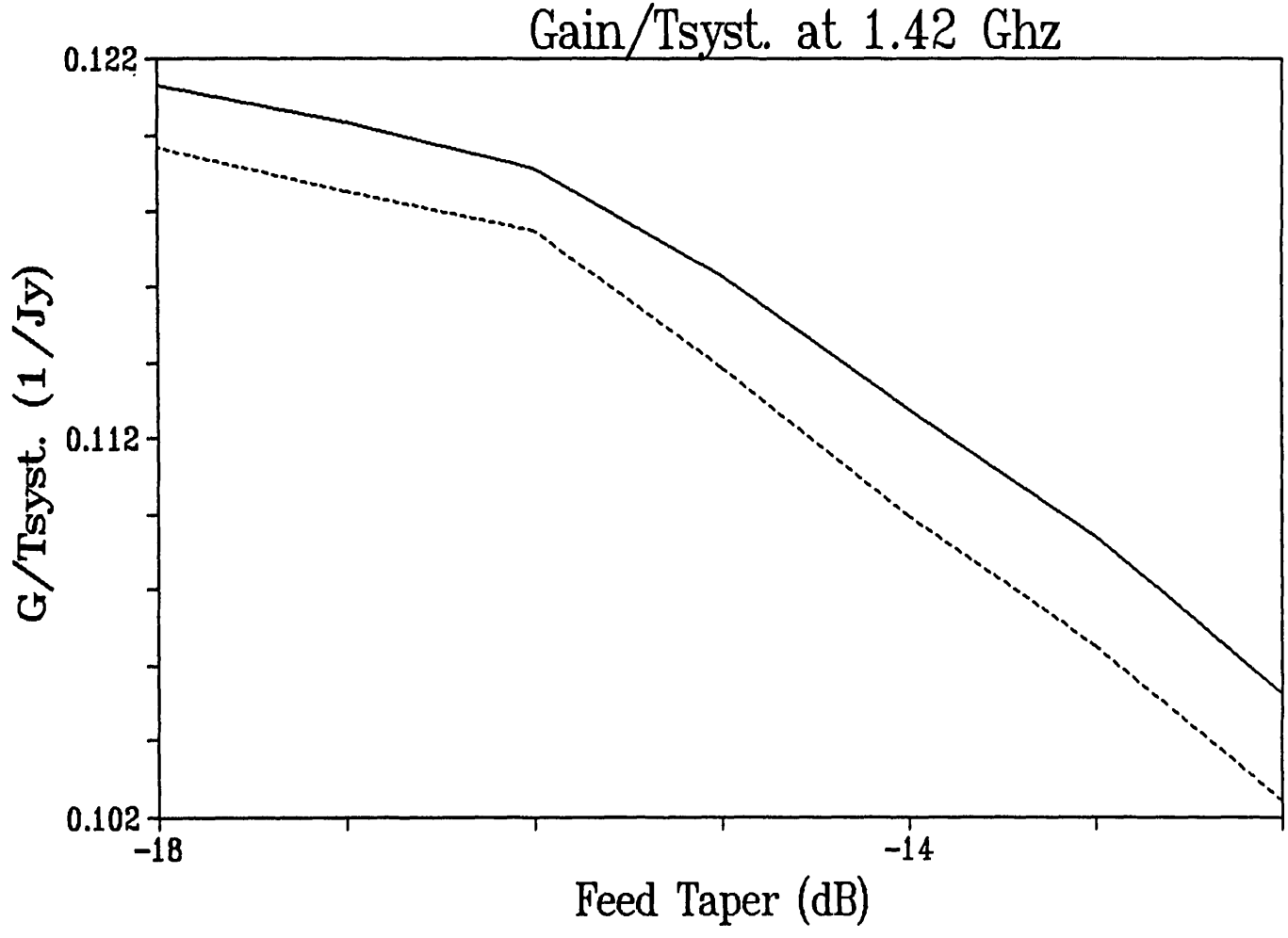
Gain/Tsyst. at 1.42 Ghz
0.122
0.112
0.102
G/Tsyst. (1/Jy)
-18
-14
Feed Taper (dB)
90 Elev.
30 Elev.

Figure 5-2

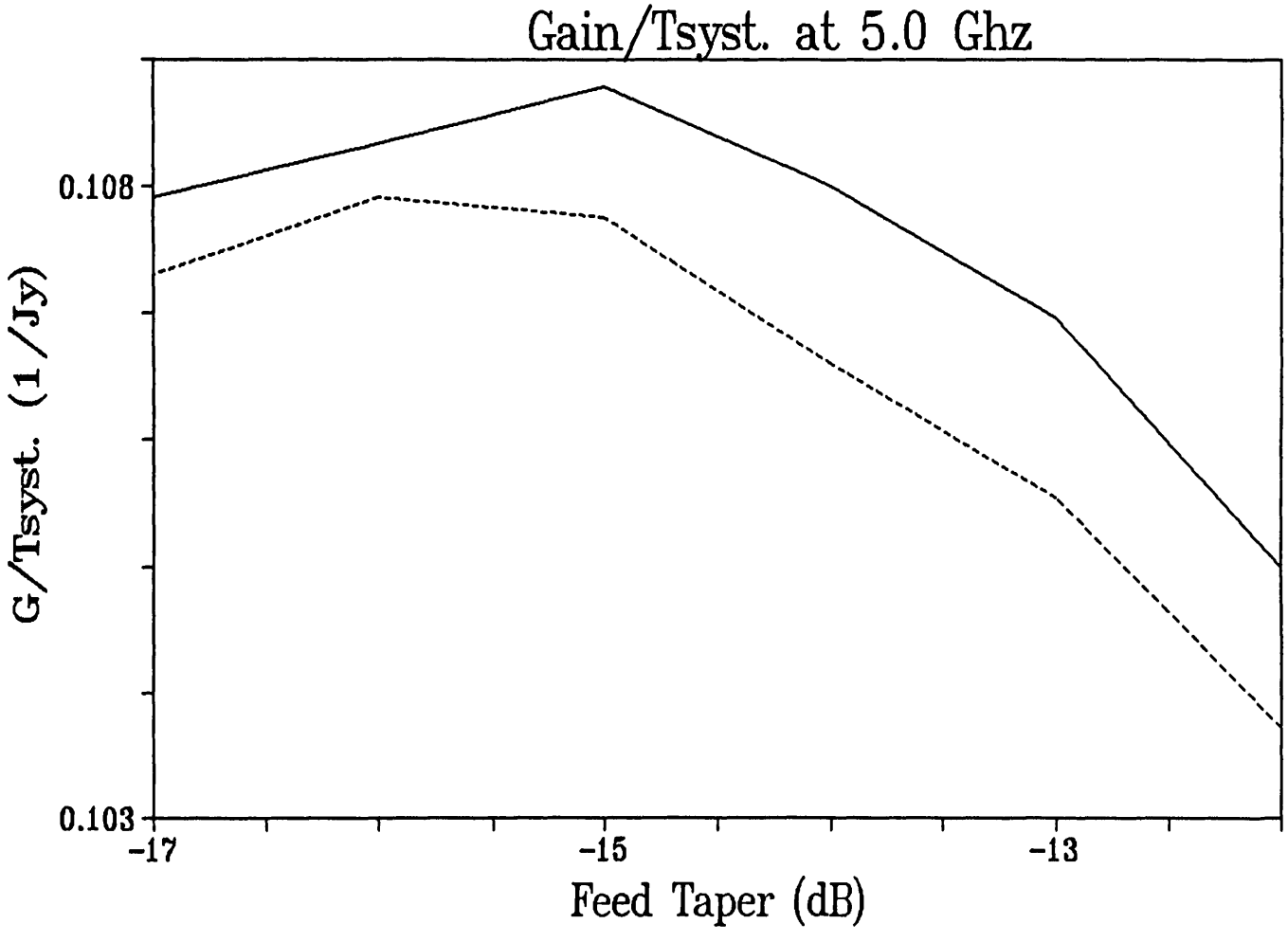
Gain/Tsyst. at 5.0 Ghz
0.108
0.103
G/Tsyst. (1/Jy)
-17
-15
-13
Feed Taper (dB)
90 Elev.
30 Elev.

Figure 5-3

Table 5-1

Freq. (GHz)	E_{main}	E_{sub}	E_{ill}	E_{tot}
1.42	0.9830	0.9039	0.8083	0.7182
5.00	0.9940	0.9039	0.8152	0.7325
20.00	0.9970	0.9039	0.8246	0.7431

Table 5-2

Freq. (GHz)	Scan Angle / *$HPBW_o$	Symmetric Plane			Asymmetric Plane		
		Loss in Gain (dB)	HPBW / $HPBW_o$	First Sidelobe Level (dB)	Loss in Gain (dB)	HPBW / $HPBW_o$	First Sidelobe Level (dB)
1.42	2.8	0.308	1.07	-28.1	0.135	1.02	-23.4
	6.0	1.125	1.21	-24.4	0.922	1.10	-20.5
5.00	2.8	0.140	1.01	-26.6	0.018	1.00	-26.8
	6.0	0.467	1.06	-25.7	0.080	1.02	-26.5
	10.0	0.789	1.13	-23.7	0.228	1.04	-26.1

*$HPBW_o$ - half power beamwidth of unscanned beam

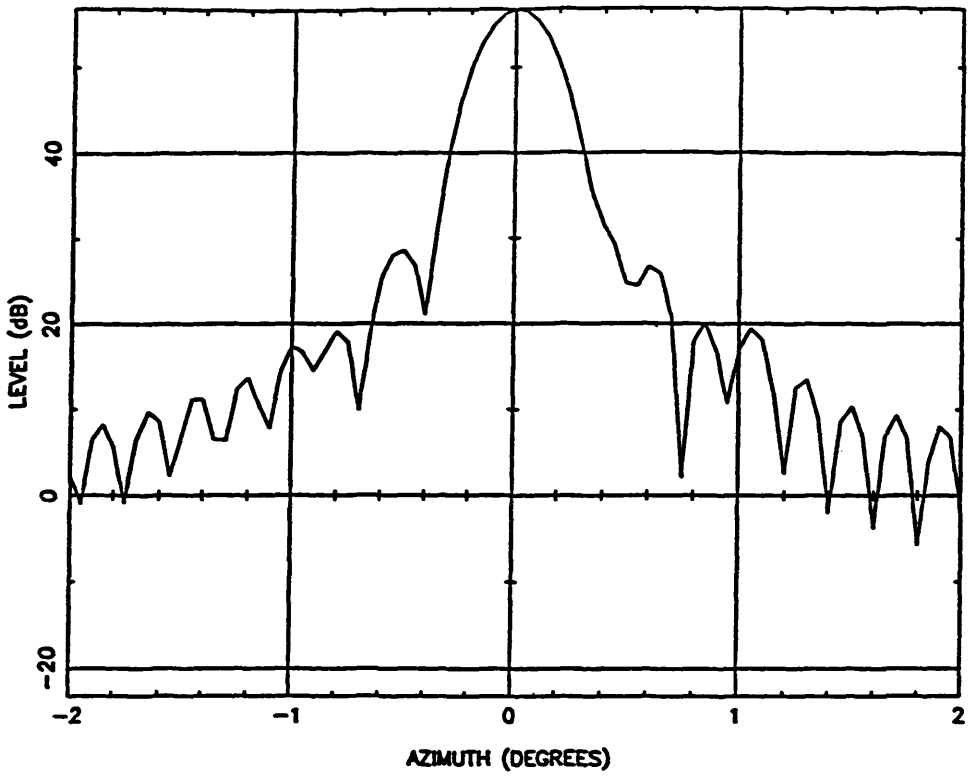

Figure 5-4 Far-field pattern at 800 MHz - Prime Focus

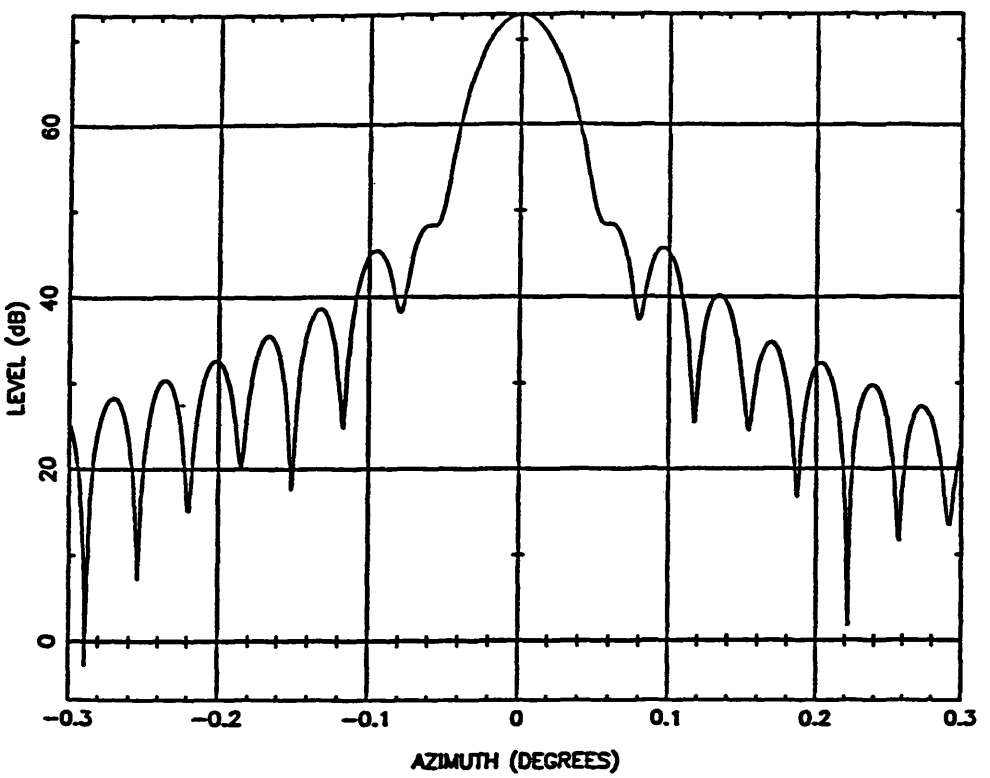

Figure 5-5 Far-field pattern at 5 GHz - Secondary Focus

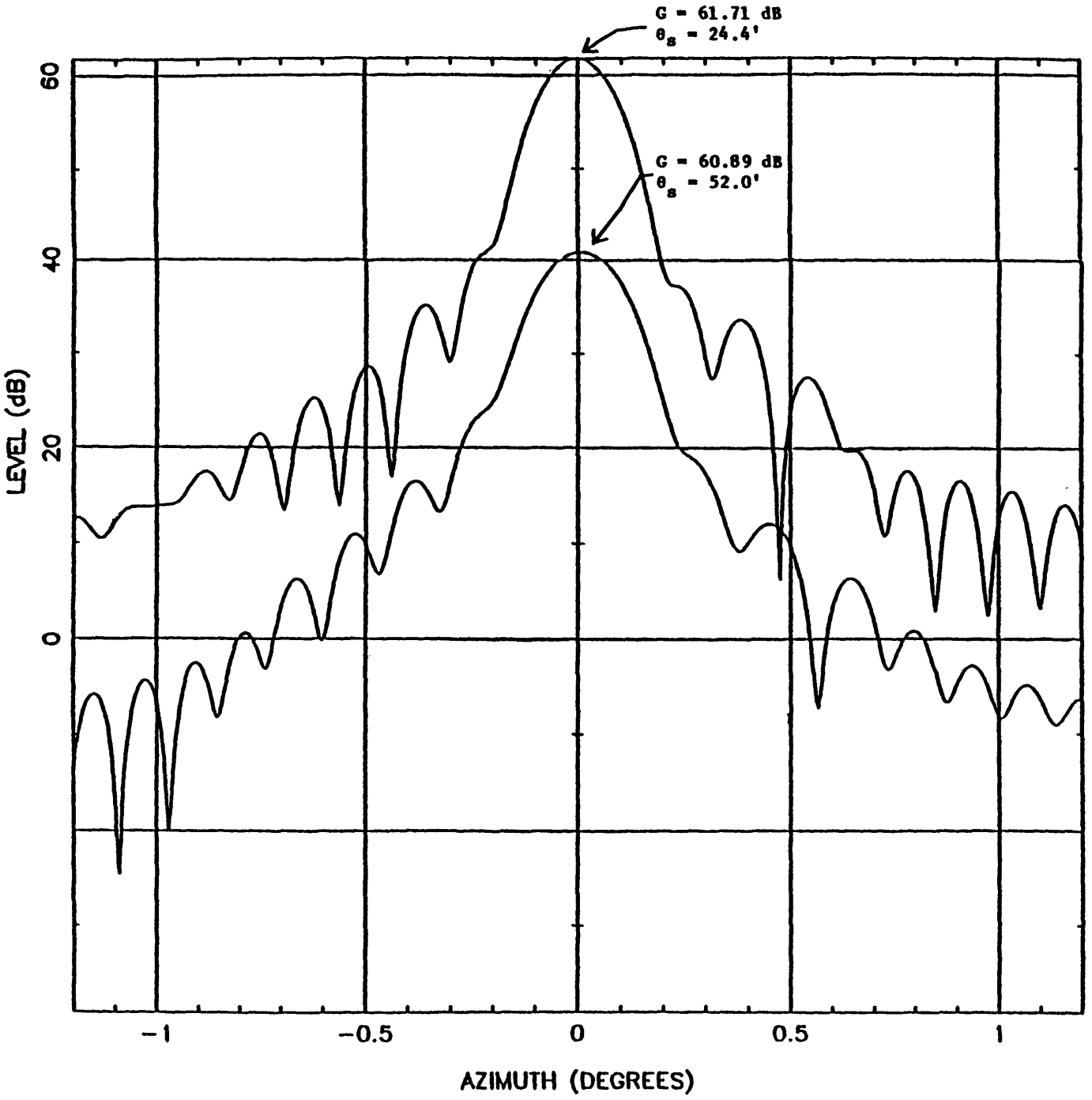

Figure 5-6 Scanned far-field patterns at 1.42 GHz.

(Plane of Symmetry)

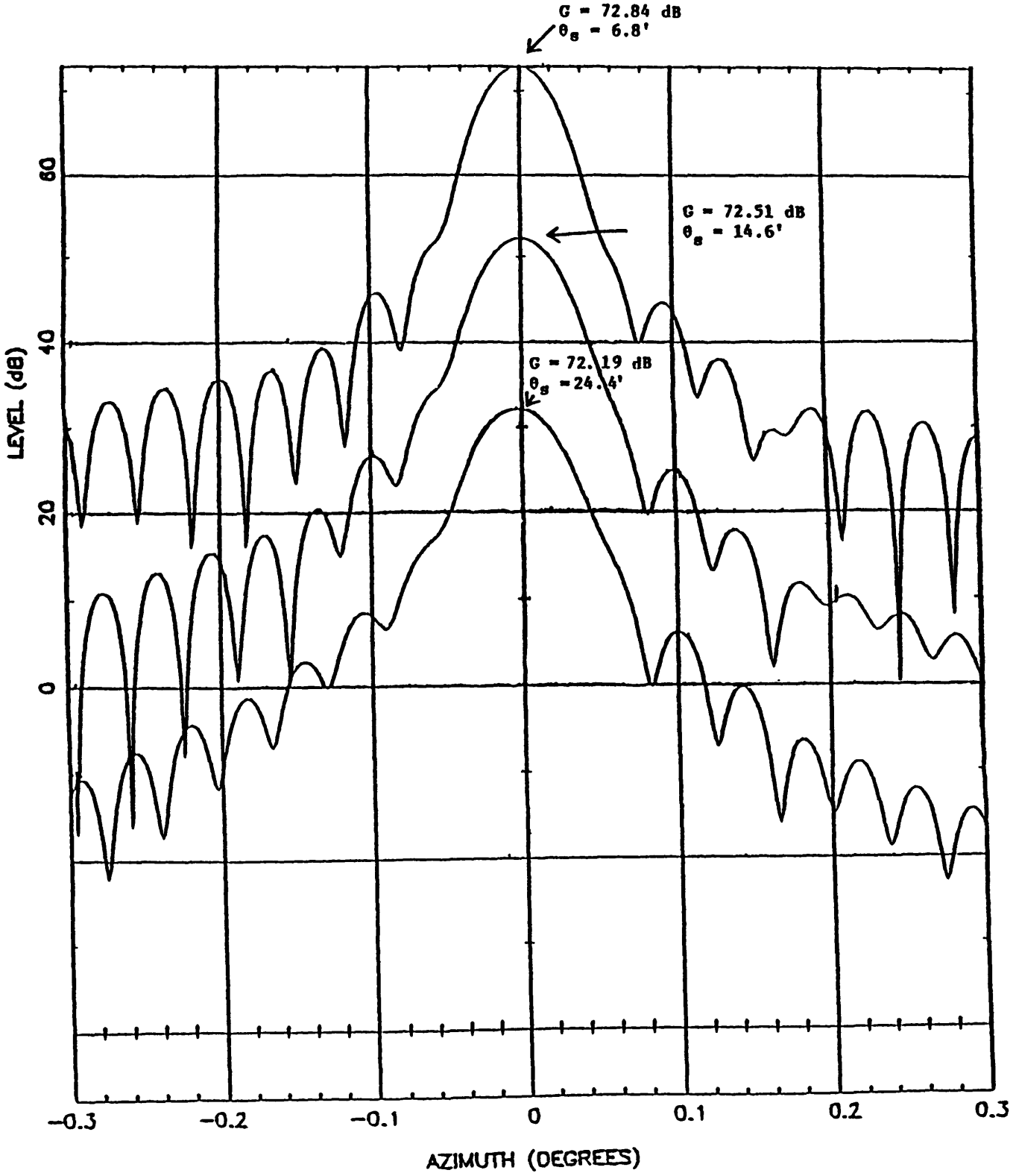

Figure 5-7 Scanned far-field patterns at 5 GHz.

(Plane of Symmetry)